11th International Symposium on Turbulence and Shear Flow Phenomena (TSFP11)
Southampton, UK, July 30 to August 2, 2019

ENTRAINMENT AND RESUSPENSION MODELING FOR SMALL INERTIAL PARTICLES IN WALL-BOUNDED TURBULENT FLOW

Ruifeng Hu
College of Civil Engineering and Mechanics,
Lanzhou University
Lanzhou 731000 China
hurf@lzu.edu.cn

Perry L. Johnson
Center for Turbulence Research
Stanford University
Stanford CA 94305 USA
perryj@stanford.edu

Charles Meneveau
Department of Mechanical Engineering
Johns Hopkins University
Baltimore MD 21218 USA
meneveau@jhu.edu

ABSTRACT

Particle entrainment into turbulent boundary layer flow is a phenomenon of great importance to many environmental and industrial processes, e.g. dust particle entrainment into the atmosphere. In this study, we extend a dynamic resuspension model for applicability to rough surfaces with multiscale roughness elements, and couple it with a DNS database of turbulent channel flow to track particle trajectories. The study aims at isolating the physical mechanisms for small inertial particle resuspension by near-wall turbulence and particle interactions with small surface roughness elements. Secondly, a simple stochastic model is developed as particle subgrid-scale (SGS) model combined with spatially filtered turbulent flow fields. Good agreements between coarse-grained simulations and DNS results have been obtained.

INTRODUCTION

Particle-laden turbulent two-phase flows are ubiquitous in nature and engineering. In many circumstances, particles are directly picked up from the wall by turbulent flow. For example, dust particles with diameter smaller than about 70 μm can be entrained by strong winds into short/long-time suspensions (Kok *et al.*, 2012). This so-called resuspension phenomenon can play an important role in sediment transport, outdoor/indoor environment, food engineering, nuclear engineering, filtration system, etc. For more detailed background, see a recent review paper by Henry & Minier (2014*a*).

A resuspension model is needed to describe how a particle interacts with a rough surface and predicts the critical condition when a particle can be picked up. There are mainly four classes of resuspension models in the literature (Henry & Minier, 2014*a*), namely the empirical model, static force-balance model, kinetic probability model and the dynamic probability model. The empirical model predicts particle resuspension rate (ratio between particle suspension flux and surface concentration) by fitting measurement data, e.g. Kim *et al.* (2010). The static force-balance model gives the critical condition at which the force balance is broken (Ibrahim *et al.*, 2003), however the rolling/sliding motion of particles along a rough surface is not included. The kinetic probability model, like the RRH model (Reeks *et al.*, 1988) or Rock'n'Roll model (Reeks & Hall, 2001), can take into account the rolling motion and kinetic energy accumulation of particles on rough surfaces. This type of model requires additional phenomenological differential equations. The dynamic probability model is directly based on the fundamental principles of Newtonian mechanics to solve the rolling motion of particle on a rough surface. For example, the stochastic dynamic model of Henry & Minier (2014*b*) divides the particle resuspension process into three steps, i.e. a particle is set into motion from a static force balance, followed by particle rolling on a surface including roughness, and then a particle hitting a large asperity so it is lifted off the surface.

Studies of resuspension models mostly focus on the critical condition when a particle can be entrained into the flow. Some attempts have been reported to couple particle resuspension model with flow simulation to examine the evolution of the particle suspension process and underlying physical mechanisms. Soltani & Ahmadi (1995) performed one-way coupled DNS study of particle entrainment and suspension in a channel flow, but all particles are initially located at $y^+ = 1$ not at the surface, hence no resuspension model was invoked. Wu *et al.* (2017) studied particle resuspension phenomenon under periodically forced impinging jet flow through wall-resolved large eddy simulation (LES), in which particles are initially put at the first grid center away from the surface. In order to sustain a continuous suspension of particles from a surface, Richter & Chamecki (2018) introduced a stochastic Brownian motion model to be equivalent with the turbulent diffusion of the particulate phase.

A key factor in particle resuspension models is to include account of surface roughness (typically much smaller than viscous scales, i.e. could be hydrodynamically smooth). We have confirmed numerically in a number of tests that inertial particle can hardly be directly picked up

by turbulent flow if placed initially on a mathematically smooth surface. In the prior dynamic model of Henry & Minier (2014*b*) such rough surface cases were modeled by assuming the presence of distinct small and large semi-spherical asperities. In the present work, we generalize the model with a hierarchy of multi-scale asperities to represent surface roughness more closely approximating naturally realistic conditions. Then we couple the generalized particle resuspension model with a time-resolved DNS database of a turbulent channel flow assuming one-way coupling. We aim to produce benchmark data for coarse-grained simulations. Lastly, we propose a stochastic particle SGS model and near-wall model, and perform coarse-grained simulations.

MODEL DESCRIPTION

Equations of Particle Motion

In our study of particle entrainment into turbulent boundary layer flow, we resort to a Lagrangian model of particle motion. We first describe the governing equations for a small inertial particle moving in an incompressible Newtonian fluid and secondly focus on the resuspension model that describes the initial pickup of particles initially located at the surface. The fluid velocity is obtained either from a DNS database or from coarse-grained simulation with a simplified stochastic model.

The Lagrangian particle trajectory is obtained from

$$\frac{d\mathbf{x}_p}{dt} = \mathbf{u}_p, \quad \frac{d\mathbf{u}_p}{dt} = \mathbf{f}_d + \mathbf{f}_l, \tag{1}$$

$$\mathbf{f}_d = \frac{k_p}{\tau_p}(\mathbf{u}_f - \mathbf{u}_p), \tag{2}$$

$$\mathbf{f}_l = J\frac{9.69}{\pi}\frac{\rho_f}{\rho_p}\frac{\nu_f}{d_p}\frac{(\mathbf{u}_f - \mathbf{u}_p)\times(\nabla\times\mathbf{u}_f)}{\sqrt{|\nabla\times\mathbf{u}_f|}}, \tag{3}$$

in which $\mathbf{x}_p$ and $\mathbf{u}_p$ are particle position and velocity vectors, $\mathbf{u}_f$ is the local fluid velocity seen by the particle, ρ_f and ρ_d are fluid and particle densities, ν_f is fluid kinematic viscosity, d_p is particle diameter, and $\mathbf{f}_d$ and $\mathbf{f}_l$ are fluid drag and shear-induced lift forces exerted on the particle. The fluid drag $\mathbf{f}_d$ is modeled through the drag law for small particle moving in an incompressible Newtonian fluid. Here small particle means its diameter is much smaller than the smallest flow length scale. $\tau_p = \rho_p d_p^2/18\mu_f$ is the particle response time scale, μ_f is fluid dynamic viscosity, and $k_p = 1 + 0.15Re_p^{0.687}$ accounts for the finite-Reynolds number correction on the fluid drag model of Stokes flow (Schiller & Naumann, 1933). $Re_p = |\mathbf{u}_f - \mathbf{u}_p|d_p/\nu_f$ is the particle Reynolds number. The aerodynamic lift is modeled according to Saffman (1965, 1968). The prefactor J accounts for the correction of Saffman's lift to finite particle Reynolds number (McLaughlin, 1991). And the approximate fitting of Mei (1992) is adopted in this study. The added-mass force, Basset history force and pressure-gradient force are not included because their effects are negligible in the regimes intended in this study. It should be noted that we neglect near-wall corrections to drag and/or lift models that may be required in further refinements of the approach.

Particle Resuspension Model

For the particle resuspension criterion from a rough wall, we generalize a dynamic stochastic particle resuspension model of Henry & Minier (2014*b*). In their original work, a rough surface is assumed to be covered by two-level small-scale and large-scale asperities. The particle resuspension process is modeled by a three-stage scenario, i.e. a particle is set in motion (stage I), followed by rolling motion along the rough surface due to fluid and adhesion forces (stage II), and finally a detachment from the wall when a particle with sufficiently high kinetic energy collides with a large-scale asperity (stage III).

The DLVO theory (Deraguin & Landau, 1941; Verwey & Overbeek, 1948) is used as the adhesion force model to calculate the Van de Waals force between particle and wall following Henry & Minier (2014*b*):

$$F_a = -\frac{dU_{rough}}{dz} \approx -\frac{U_{rough}(z_0+\varepsilon) - U_{rough}(z_0)}{\varepsilon}, \tag{4}$$

where $z_0 = 0.165$ nm, $\varepsilon = 10^{-11}$ m, and U_{rough} is the interaction energy between a particle and a rough wall, i.e.

$$U_{rough} = U_{smooth} + \sum_{i=1}^{N_{asp}} U_{i,p-a}, \tag{5}$$

in which U_{smooth} is the interaction energy between a particle and a smooth wall, which is detailed in Henry *et al.* (2012). U_{p-a} is the interaction energy between a particle and an asperity, modeled by

$$U_{p-a}(h) = -\frac{A_H R_p R_a}{6h(R_p+R_a)}\left[1 - \frac{5.32h}{\lambda}\ln\left(1+\frac{\lambda}{5.32h}\right)\right]. \tag{6}$$

A_H is the Hamaker constant, λ is a characteristic wavelength for retardation effects and set to 100 nm.

The adhesion moment acting on a particle is then

$$M_a = F_a a_0. \tag{7}$$

The pivot distance a_0 is defined as the relevant moment arm from interactions with the furthest small-scale asperity contacting with the particle in downstream, which is given by a probability with uniform distribution. The number of asperities contacting with a particle N_{asp} is stochastically generated by a Poisson distribution.

The equation of rolling motion of a particle along the wall is calcuated following Henry & Minier (2014*b*)

$$I_p\dot{\omega}_p = M_d + M_a, \tag{8}$$

$$M_d = 1.4 f_d R_p, \tag{9}$$

$$f_d = 6\pi f \mu_f R_p(u_f - u_p), \tag{10}$$

in which, I_p is the moment of inertia of particle around the pivot point, ω_p is the angular velocity of the particle, $u_p = \omega_p R_p$ is the translation velocity of the particle in purely rolling motion, M_d is the fluid-induced moment in the streamwise direction, and $f = 1.7$ is a factor accounting for wall correction effect Henry & Minier (2014*b*).

Since the introduction of distinct small-scale and large-scale asperities is arbitrary in Henry & Minier (2014*b*), we generalize their model by introducing a multiscale, fractal-like rough wall (Anderson & Meneveau, 2011) with a hierarchy of asperity sizes. The distribution follows $D_{n+1} =$

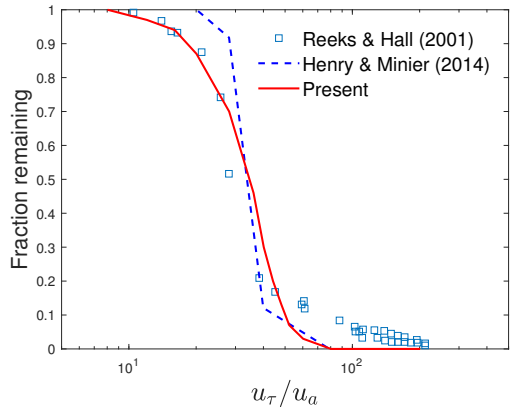

Figure 1. Fraction of particles remaining on the wall after 1 s exposure to airflow with varying wind friction velocity u_τ. $u_a = \sqrt{\sigma A_H/m_p}$ is a reference velocity scale, where density ratio $\sigma = \rho_p/\rho_f$ is set to be 1600, the Hamaker constant $A_H = 2.5\times10^{-19}$ J, and m_p is the mass of the particles. The particle radius is 5 μm, the minimum and maximum asperity radii are 5 nm and 2 μm respectively, and the number of asperity levels is set to 10.

$2^{-n}D_1$, where D_n is the nth-level asperity size. With a constant coverage area for different asperity sizes, the number density of asperity in each level obeys a D^{-2} power law, as $N(D_n)\sim D_n^{-2}$. In the present study, we define the large-scale asperities responsible for resuspension as having $D_n \geq d_p/100$. Then if a particle hits a large-scale asperity, the resuspension criterion is whether its kinetic energy is higher than the adhesion well, i.e. $E_k = m_p U_p^2/2 > U_{p-a}(z_0)$ (m_p is the mass of a particle), and the particle will be lifted off at a vertical velocity equivalent to the streamwise one before the collision (assuming elastic collision).

As a first application of the model, we consider fluid velocities generated from the stochastic model of (Henry & Minier, 2014*b*). Figure 1 shows a comparison of the remaining particle fraction on the wall after 1 second exposure to airflow between predictions of the stochastic resuspension model with experimental data of Reeks & Hall (2001). It is seen that the prediction by the present generalized model is in better agreement with the experimental data than the original model of Henry & Minier (2014*b*), especially at small wind friction velocities. It should be noted again that although the wall is covered by asperities, their sizes are much smaller than the viscous scale, i.e. $D^+_{max} \ll 1$, thus the smooth-wall hydrodynamic assumption is still valid.

Subgrid-Scale and Near-Wall Models

We propose a simple stochastic particle subgrid-scale (SGS) model in coarse-grained simulation aiming to recover the flow velocity seen by a particle which is needed in the equations of particle motion.

The proposed stochastic model is a modified Ornstein-Uhlenbeck-type process, which is

$$du'_{f,i} = -\frac{u'_{f,i}}{T^*_{L,i}}dt + \sqrt{\frac{2}{T^*_{L,i}}}dM_i, \tag{11}$$

where, $u'_{f,i}$ is the SGS flow velocity component along a particle's trajectory in the ith direction. In the diffusion term, $dM_i = L_{i,j}dW_j$ and dW_j is a vector Wiener process ($\langle dW_i\rangle$=0 and $\langle dW_i dW_j\rangle = \delta_{ij}dt$), in which $L_{i,j}$ is determined by the Cholesky decomposition $L_{ij}L_{ji} = C_{ij} = \langle u_{f,i}u_{f,j}\rangle - \langle \tilde{u}_{f,i}\tilde{u}_{f,j}\rangle$, in which $\tilde{u}_{f,i} = u_{f,i} - u'_{f,i}$ is the resolved flow velocity component. The Lagrangian time scales in the longitudinal direction ($i=1$) and transverse directions ($i=2$ and 3) are given by

$$T^*_{L,1} = \frac{T_{SGS}}{\sqrt{1+\beta^2\frac{|\tilde{\mathbf{u}}_r|^2}{2k_{SGS}/3}}}, \tag{12}$$

$$T^*_{L,2} = T^*_{L,3} = \frac{T_{SGS}}{\sqrt{1+4\beta^2\frac{|\tilde{\mathbf{u}}_r|^2}{2k_{SGS}/3}}}, \tag{13}$$

$$T_{SGS} = \frac{k_{SGS}}{\Pi}\left(\frac{1}{2}+\frac{3}{4}C_0\right)^{-1}, \tag{14}$$

in which Π is the kinetic energy transfer rate from resolved to unresolved scale computed from $\Pi = (C_s\Delta)|\tilde{\mathbf{S}}|^3$ using a Smagorinsky SGS model, C_s is assumed to be 0.19 in filtered DNS cases, Δ is the filter size and $|\tilde{\mathbf{S}}| = \sqrt{2\tilde{S}_{ij}\tilde{S}_{ij}}$ is the modulus of resolved velocity gradient tensor $\tilde{S}_{ij}$. $|\tilde{\mathbf{u}}_r|$ is the modulus of the relative velocity between particle and flow. k_{SGS} is the SGS kinetic energy modeled as $k_{SGS} = C_\varepsilon(\Delta\Pi)^{2/3}$ with $C_\varepsilon = 1.65$ (Innocenti *et al.*, 2016; Johnson & Meneveau, 2018). Other model constants are given as $C_0 = 2.1$ and $\beta = 0.8$ (Pope, 1994; Minier & Peirano, 2001; Innocenti *et al.*, 2016; Johnson & Meneveau, 2018).

The grid resolution is very coarse in the heavily modeled simulation to be considered in the present work, so that the near-wall region is not resolved. This leads to the requirement for a near-wall model of flow velocity and velocity gradient. In a preliminary attempt, we use piecewise functions to explicitly enrich the resolved streamwise and spanwise velocity components in the viscous and logarithmic layers below the first grid off the wall (which we assume is at height y_1), following the general idea of the integral wall model (Yang *et al.*, 2015). In the viscous layer (including some part of buffer layer), i.e. $y^+ \leq \min(11, y_1^+)$, we use the linear velocity profile, as

$$\tilde{u}_{f,x} = \frac{\tilde{\tau}_{w,x}}{\mu_f}y, \quad \tilde{u}_{f,z} = \frac{\tilde{\tau}_{w,z}}{\mu_f}y, \tag{15}$$

$$\frac{\partial\tilde{u}_{f,x}}{\partial y} = \frac{\tilde{\tau}_{w,x}}{\mu_f}, \quad \frac{\partial\tilde{u}_{f,z}}{\partial y} = \frac{\tilde{\tau}_{w,z}}{\mu_f}, \tag{16}$$

here $\tilde{\tau}_{w,x}$ and $\tilde{\tau}_{w,z}$ are streamwise and spanwise resolved wall-shear stress, respectively.

In the logarithmic layer (also including some part of buffer layer), i.e. $\min(11, y_1^+) < y^+ < y_1^+$, we adopt the classical logarithmic velocity law, as

$$\tilde{u}_{f,x} = \tilde{u}_{\tau,x}\left(\frac{1}{\kappa}\ln y^+ + B\right), \tag{17}$$

$$\tilde{u}_{f,z} = \tilde{u}_{\tau,z}\left(\frac{1}{\kappa}\ln y^+ + B\right), \tag{18}$$

$$\frac{\partial\tilde{u}_{f,x}}{\partial y} = \frac{\tilde{u}_{\tau,x}}{\kappa y}, \quad \frac{\partial\tilde{u}_{f,z}}{\partial y} = \frac{\tilde{u}_{\tau,z}}{\kappa y}, \tag{19}$$

in which, $\tilde{u}_{\tau,x} = \sqrt{\tilde{\tau}_{w,x}/\rho_f}$ and $\tilde{u}_{\tau,z} = \sqrt{\tilde{\tau}_{w,z}/\rho_f}$ are streamwise and spanwise resolved friction velocity components,

respectively. And model constants are set to $\kappa = 0.41$ and $B = 5.2$.

NUMERICAL DETAILS

For more detailed testing of the model, we use fluid velocities from DNS. Specifically, we use the turbulent channel flow dataset at $Re_\tau = 1000$ available from JHTDB (Graham *et al.*, 2016) as the background flow to compute the particle motion in the one-way coupled way. The channel flow dataset is produced by a direct numerical simulation (DNS) in a wall-normal velocity-vorticity form using a pseudo-spectral method in the horizontal plane and a seventh-order B-splines collocation method in the wall-normal direction (Lee *et al.*, 2013). Dealiasing is performed using the 3/2-rule. Temporal integration is performed using a low-storage, third-order Runge-Kutta method. The simulation domain size is $8\pi \times 2 \times 3\pi$ with a spatial resolution of $2048 \times 512 \times 1536$ in the streamwise (x), wall-normal (y) and spanwise (z) directions respectively. In total 4,000 snapshots in a flow through time are available.

To mimic a large-eddy simulation (LES), we also filtered the DNS channel flow data using a trapezoidal rule with a box filter size of 64 times the grid spacing, which is twice coarser than the one used by Johnson & Meneveau (2018), e.g. $\Delta_x = 64\delta_x$, where Δ_x and δ_x are filter width and DNS grid spacing in the x direction, respectively. The filtering is similar in y and z directions. Every 32 snapshot was filtered in time and thus temporal resolution is 32 times coarser. The size of the coarse-grained dataset was $64 \times 16 \times 48$ with 125 time steps.

The equations of particle motion are numerically solved by a second-order Adams-Bashforth scheme. We also compared the result with that using fourth-order Runge-Kutta scheme, with negligible differences. The trajectories by both schemes almost coincide with each other at $\Delta s/d_p$ up to $O(10^5)$, where Δs is the trajectory length. And there are only marginal differences in the particle concentration distribution. In the DNS study, the local flow velocity at the particle position is obtained by the built-in *getVelocity* function in JHTDB using a sixth-order Lagrange spatial interpolation and a third-order Hermite polynomial temporal interpolation. The time step for particle motion integration is $dt_p^+ = dt_p/(\nu_f/u_\tau^2) \approx 0.1$. In the filtered-DNS study, the flow velocity is interpolated linearly in both space and time. In this study, initially 10,000 particles are put on the wall at rest with a uniformly random planar distribution. If a particle crosses the center plane of the channel, it is reseeded on the wall, thus only one half of the channel flow data is used. The particle Stokes number, here defined as $St = \tau_p/\tau_\nu$ ($\tau_\nu = \nu_f/u_\tau^2$) in viscous units, is set to be 5, 30 and 100, corresponding to viscous-scaled particle diameters of $d_p^+ = 0.27$, 0.66 and 1.21 respectively. For reference, if we set a dimensional friction velocity of $u_\tau = 1$ m/s for all three kinds of particles and use air viscosity $\nu = 1.5 \times 10^{-5}$ m^2/s, then the channel half-width is $H \approx 0.16$ m, and the dimensional particle diameters are around 4.2 μm, 10.4 μm and 19.0 μm.

RESULTS

DNS Results

Figure 2 displays the time evolution of the Shannon entropy of the particle distribution using the model with and without including the lift force term. The Shannon entropy

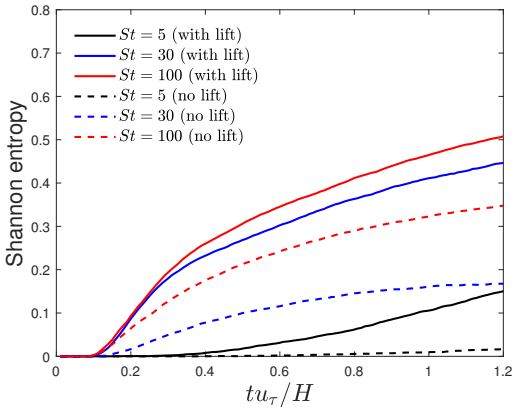

Figure 2. Temporal variation of Shannon entropy characterizing the spatial distribution of particles after one flow-through-time of channel flow using DNS.

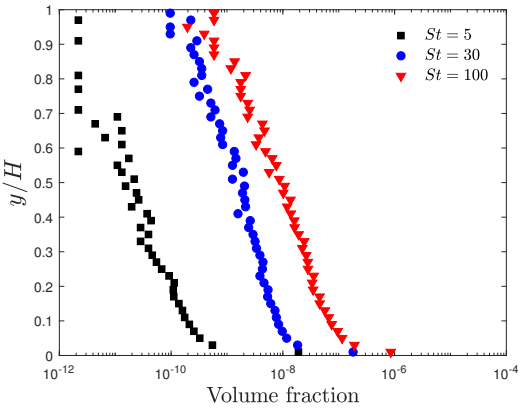

Figure 3. Particle volume fraction distribution at $tu_\tau/H \approx 1.29$ from DNS by including lift, as function of distance to the wall from where the particles are being entrained, for various particle Stokes numbers.

is defined by $S = P/\ln N_s$, with $P = -\sum_{j=1}^{N_s} p_j \ln p_j$, where p_j is the probability density of finding the particle in the jth bin, N_s is the total number of bin used to discretize the wall-normal direction. Here we subdivide the entire channel height into 100 bins, uniformly. The Shannon entropy S is a useful parameter to quantify the vertical preferential concentration of particle distribution (Picano *et al.*, 2009), with $S = 1$ for uniform distribution and $S = 0$ for the extreme non-uniform case of all particles in one bin. After one flow through time, a fraction of particles are picked up from the wall and are entrained into the flow. In the limited time duration of the dataset, we can see that the particle distribution is still developing and a statistically stationary state has not been achieved. But the present result could be useful as benchmark data for further model validation. It is also clearly evident that the lift plays an important role in particle resuspension. Figure 3 shows the probability density of particle distribution at $tu_\tau/H \approx 1.29$ (after one flow through time) in the wall-normal direction, by including the lift force. In general, in the bulk of the channel, the number of particles with higher inertia is larger because particles with higher inertia are easier to be picked up by the flow, as shown in figure 1.

Coarse-Grained Simulation Results

As a first test, we perform simulation of the evolution of inertia-less tracer particles ($\tau_p = 0$) in the channel flow using the filtered DNS (fDNS) data coupled with the particle SGS model, and totally 10,000 particles are uniformly distributed across the channel at $t = 0$. The particle probability density function (PDF) distribution is expected to remain uniform with y at any instant. Figure 4 (a) displays the PDF of the tracer particles y-position after one flow-through time. It is seen that the PDF is close to the target value $1/N_s$ through the channel height, with slightly higher values in the channel center and very close to the walls, and slightly lower than $1/N_s$ at $y \approx -0.9$ and 0.9 ($y^+ \approx 100$). This is because the strongest wall-normal velocity fluctuations occur at $y^+ \approx 100$, see figure 4 (c). The particle-sampled mean streamwise flow velocity is in very good agreement with the DNS result, as shown in figure 4 (b). The flow velocity fluctuations are somewhat overestimated in all directions from sampling result of the tracer particles, especially near their peaks. However the streamwise and wall-normal fluctuating velocity covariance $\langle uv \rangle$ is reasonably predicted by the fDNS coupled with the particle SGS model.

Figure 5 shows a comparison of particle volume fraction distribution at $tu_\tau/H \approx 1.29$ between DNS, fDNS, and fDNS coupled with the particle SGS model or/and the near-wall model. In general, we can observe that the fDNS coupled with both the particle SGS model and the near-wall model yields the best results, and the fDNS without any model produces the worst predictions, in all cases with different particle Stokes number as well as including lift or not. The results appear reasonable since the entrainment and resuspension of the particles are highly dependent on near-wall turbulence, and the near-wall model provides improved resolved streamwise velocity and velocity gradient representations. On the other hand, the predictive capability of the model also strongly depends on the particle Stokes number. For example, if not including lift, no particle is predicted to be picked up by the coarse-grained simulation at $St = 5$, as shown in figure 5 (a). However, particles with $St = 100$ can be predicted to be successfully entrained into the flow by the fDNS coupled with the particle SGS model and/or the near-wall model, although it is still underestimated, as seen in figure 5 (c). This is because the particles with smaller inertia are more responsive to small-scale velocity fluctuations which have been filtered out in the coarse-grained simulation. In Figs. 5 (a-d), several of the cases are not visible as particles remain at the wall and their volume fraction is represented by a single symbol at $y = 0$.

The agreement between the coarse-grained simulation and the DNS results is seen to be much better if we include the lift force, which can be ascribed to the more important role of the lift played as well as the visible improvement by the near-wall model. The preliminary results shown in figure 5 imply that there still is room for significant improvements of the coarse-grained simulation models, especially at small particle Stokes number. One possible idea is to separately take into account the positive and negative wall-normal fluid motions (sweep and ejection events) in the particle SGS model, since stronger ejection events can help more particles to be lifted up. And the near-wall model could also be improved by including the wall-normal velocity component explicitly.

SUMMARY

In this study, we numerically solved the equations of particle motion with a resuspension model to simulate entrainment of small inertial particles by near-wall turbulent flow. The resuspension model of Henry & Minier (2014*b*) is generalized to a more realistic rough surface geometry with more length-scales present, leading to results that agree better with experimental data. Then, particle motion is coupled with channel flow DNS assuming one-way coupling. The preliminary results demonstrate the importance of including aerodynamic lift and highlight the strong effects of particle inertia. We also conducted coarse-grained particle simulations (with filtered DNS fluid velocities) of this problem, with a simple particle SGS model and near-wall model. Further refinements and optimizations of these models could yield predictions in better agreement with the DNS result.

Acknowledgements: RH thanks the CSC scholarship and NSFC funding (11490553). CM acknowledges partial funding from NSF (CBET-1738918).

REFERENCES

Anderson, W. & Meneveau, C. 2011 Dynamic roughness model for large-eddy simulation of turbulent flow over multiscale, fractal-like rough surfaces. *J. Fluid Mech.* **679**, 288–314.

Deraguin, B. V. & Landau, L. 1941 Theory of the stability of strongly charged lyophobic sols and of the adhesion of strongly charged particles in solution of electrolytes. *Acta Physicochim: USSR* **14**, 633–662.

Graham, J., Kanov, K., Yang, X. I. A., Lee, M., Malaya, N., Lalescu, C. C., Burns, R., Eyink, G., Szalay, A., Moser, R. D. & Meneveau, C. 2016 A web services accessible database of turbulent channel flow and its use for testing a new integral wall model for les. *J. Turbul.* **17** (2), 181–215.

Henry, C. & Minier, J.-P. 2014*a* Progress in particle resuspension from rough surfaces by turbulent flows. *Prog. Energy Combust. Sci.* **45**, 1–53.

Henry, C. & Minier, J. P. 2014*b* A stochastic approach for the simulation of particle resuspension from rough substrates: Model and numerical implementation. *J. Aerosol Sci.* **77**, 168–192.

Henry, C., Minier, J.-P. & Lefevre, G. 2012 Numerical study on the adhesion and reentrainment of nondeformable particles on surfaces: the role of surface roughness and electrostatic forces. *Langmuir* **28** (1), 438–452.

Ibrahim, A. H., Dunn, P. F. & Brach, R. M. 2003 Microparticle detachment from surfaces exposed to turbulent air flow: controlled experiments and modeling. *J. Aerosol Sci.* **34** (6), 765–782.

Innocenti, A., Marchioli, C. & Chibbaro, S. 2016 Lagrangian filtered density function for LES-based stochastic modelling of turbulent particle-laden flows. *Phys. Fluids* **28** (11), 115106.

Johnson, P. L. & Meneveau, C. 2018 Predicting viscous-range velocity gradient dynamics in large-eddy simulations of turbulence. *J. Fluid Mech.* **837**, 80–114.

Kim, Y., Gidwani, A., Wyslouzil, B. E. & Sohn, C. W. 2010 Source term models for fine particle resuspension from indoor surfaces. *Build. Environ.* **45** (8), 1854–1865.

Kok, J. F., Parteli, E. J., Michaels, T. I. & Karam, D. B. 2012 The physics of wind-blown sand and dust. *Reports on Progress in Physics* **75** (10), 1660–1669.

Lee, M., Malaya, N. & Moser, R. D. 2013 Petascale direct

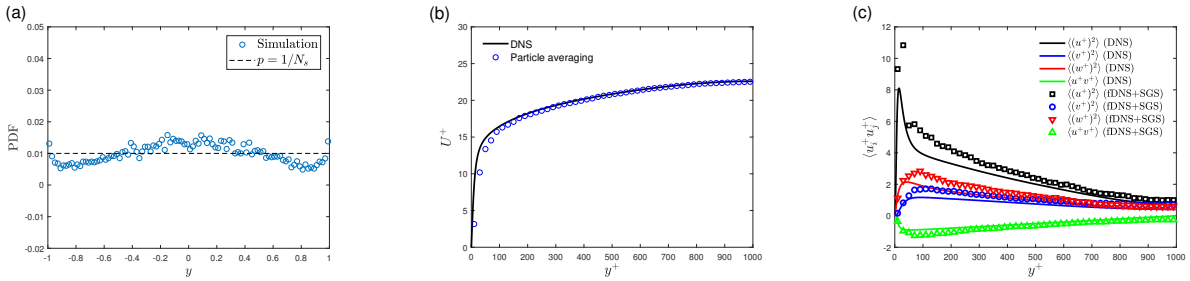

Figure 4. Test results for inertia-free tracer particles: (a) probability density function of vertical position (or particle mean concentration), (b) particle-averaged streamwise velocity profile and (c) particle-averaged fluctuating velocity Reynolds stress components.

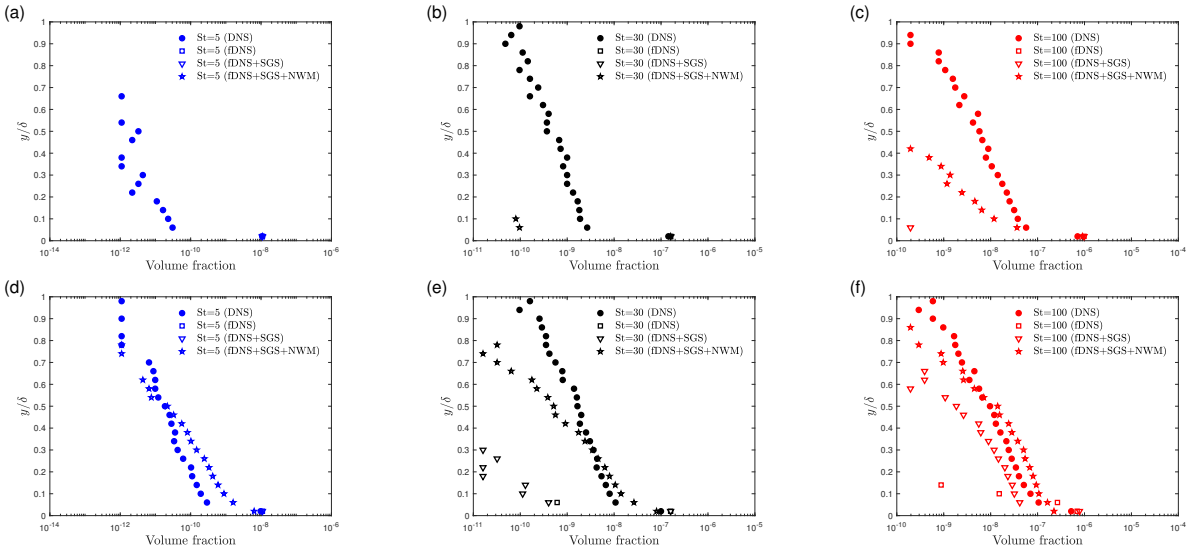

Figure 5. Comparison of particle volume fraction after one flow-through time by DNS, filtered DNS (fDNS), filtered DNS coupled with particle SGS model (fDNS+SGS) and filtered DNS coupled with both particle SGS model and near-wall model (fDNS+SGS+NWM). Subfigures (a-c) are the cases not including lift force, and (d-f) are the ones including lift force.

numerical simulation of turbulent channel flow on up to 786k cores. In *International Conference for High Performance Computing, Networking, Storage and Analysis*. New York, NY: ACM Press.

McLaughlin, J. B. 1991 Inertial migration of a small sphere in linear shear flows. *J. Fluid Mech.* **224**, 261–274.

Mei, R. 1992 An approximate expression for the shear lift force on a spherical particle at finite Reynolds number. *Int. J. Multiph. Flow* **18** (1), 145–147.

Minier, J.-P. & Peirano, E. 2001 The PDF approach to turbulent polydispersed two-phase flows. *Phys. Rep.* **352** (1-3), 1–214.

Picano, F., Sardina, G. & Casciola, C. M. 2009 Spatial development of particle-laden turbulent pipe flow. *Phys. Fluids* **21** (9), 093305.

Pope, S. B. 1994 Lagrangian pdf methods for turbulent flows. *Annu. Rev. Fluid Mech.* **26** (1), 23–63.

Reeks, M. W. & Hall, D. 2001 Kinetic models for particle resuspension in turbulent flows: theory and measurement. *J. Aerosol Sci.* **32** (1), 1–31.

Reeks, M. W., Reed, J. & Hall, D. 1988 On the resuspension of small particles by a turbulent flow. *J. Phys. D: Appl. Phys.* **21** (4), 574.

Richter, D. & Chamecki, M. 2018 Inertial effects on the vertical transport of suspended particles in a turbulent boundary layer. *Bound.-Layer Meteor.* **167** (2), 235–256.

Saffman, P. G. 1965 The lift on a small sphere in a slow shear flow. *J. Fluid Mech.* **22** (2), 385–400.

Saffman, P. G. 1968 Corrigendum to'the lift on a small sphere in a slow shear flow'. *J. Fluid Mech.* **31**, 624.

Schiller, L & Naumann, A 1933 Über die grundlegenden berechnungen bei der schwerkraftaufbereitung. *Verein. Deutsch. Ing.* **77**, 318–320.

Soltani, M. & Ahmadi, G. 1995 Direct numerical simulation of particle entrainment in turbulent channel flow. *Phys. Fluids* **7** (3), 647–657.

Verwey, E. J. W. & Overbeek, J. T. G. 1948 *Theory of the stability of lyophobic colloids*. New York: Elsevier Publishing Company.

Wu, W., Soligo, G., Marchioli, C., Soldati, A. & Piomelli, U. 2017 Particle resuspension by a periodically forced impinging jet. *J. Fluid Mech.* **820**, 284–311.

Yang, X. I. A., Sadique, J., Mittal, R. & Meneveau, C. 2015 Integral wall model for large eddy simulations of wall-bounded turbulent flows. *Phys. Fluids* **27**, 025112.